

MuSE-SVS: Multi-Singer Emotional Singing Voice Synthesizer that Controls Emotional Intensity

Sungjae Kim, Yewon Kim, Jewoo Jun, and Injung Kim

Abstract—We propose a multi-singer emotional singing voice synthesizer, Muse-SVS, that expresses emotion at various intensity levels by controlling subtle changes in pitch, energy, and phoneme duration while accurately following the score. To control multiple style attributes while avoiding loss of fidelity and expressiveness due to interference between attributes, Muse-SVS represents all attributes and their relations together by a joint embedding in a unified embedding space. Muse-SVS can express emotional intensity levels not included in the training data through embedding interpolation and extrapolation. We also propose a statistical pitch predictor to express pitch variance according to emotional intensity, and a context-aware residual duration predictor to prevent the accumulation of variances in phoneme duration, which is crucial for synchronization with instrumental parts. In addition, we propose a novel ASPP-Transformer, which combines atrous spatial pyramid pooling (ASPP) and Transformer, to improve fidelity and expressiveness by referring to broad contexts. In experiments, Muse-SVS exhibited improved fidelity, expressiveness, and synchronization performance compared with baseline models. The visualization results show that Muse-SVS effectively express the variance in pitch, energy, and phoneme duration according to emotional intensity. To the best of our knowledge, Muse-SVS is the first neural SVS capable of controlling emotional intensity.

Index Terms—singing voice synthesis, unified embedding space, statistical pitch predictor, context-aware duration predictor, ASPP-Transformer, speech processing, deep learning

I. INTRODUCTION

A singing voice synthesis (SVS) model is a generative model that produces singing voices from the lyrics, note pitch, and note duration of a music score. Similar to text-to-speech (TTS), SVS converts texts (lyrics) into speech signals. Moreover, SVS has an additional requirement of synthesizing voices according to the pitch and duration of the notes. In the past, most SVS systems were based on traditional approaches such as a concatenative method and a hidden Markov model (HMM) [1]–[3]. Recently, end-to-end neural SVS has been actively studied [4]–[9]. Neural SVS is more flexible than conventional methods and can effectively express various singing styles.

Reflecting the singer’s characteristics and emotions is important for synthesizing natural and expressive singing voices. In particular, the intensity of emotion, as well as the type, is crucial in conveying the feeling of a song. However, there are few studies on expressing emotions in SVS, and they are

based on traditional methods such as HMM [10]. To the best of our knowledge, there is no prior neural SVS model that expresses emotions of varying intensities [11]. Regarding TTS, many studies have been conducted to express emotional types [12]–[18], but there are few studies on expressing emotional intensities [18]–[20]. The main challenge in speaker/singer ID and emotion control is disentangling them from other attributes such as pitch and rhythm. In particular, expressing emotions in SVS is more challenging than in TTS as the singing voice should accurately follow the pitch and duration of notes.

Previous studies have shown that emotions in a singing voice are mainly expressed by subtle changes in a fundamental frequency (F0) contour, power envelopes, and spectral sequences [21]–[23]. Additionally, [24] reported that the level of loudness, the change in loudness, and the variations in F0 have a significant effect on emotional expression. Consequently, to effectively express emotions in a singing voice, it is essential to precisely model the variances in pitch, energy, and phoneme duration according to the type and intensity of the emotions. However, it is challenging to synthesize such variances while maintaining accurate pronunciation and following the pitch and duration of notes. Multi-singer emotional SVS is even more challenging because the model should express the timbre of multiple singers in addition to the aforementioned attributes.

In this paper, we propose Muse-SVS, the first multi-singer emotional neural SVS model that effectively expresses the type and intensity of emotions. Muse-SVS synthesizes spectrograms in a non-autoregressive manner. Muse-SVS learns each style attribute by a residual embedding conditional on the preceding attributes to reflect the correlation between style attributes, thereby avoiding interference between them. More importantly, it predicts subtle variances in pitch, energy, and phoneme duration according to the emotions while accurately following the pitch and duration of notes. Muse-SVS learns a continuous emotion embedding space and can express emotional intensities not included in the training data, including stronger emotions than those in the training data, by applying emotion embedding interpolation and extrapolation. We also propose a novel ASPP-Transformer that combines atrous spatial pyramid pooling (ASPP) [25] and Transformer [26]. The ASPP-Transformer incorporates broad contexts while focusing on local details, thereby improving the fidelity of singing voices with a large variation in phoneme duration.

To train and evaluate Muse-SVS, we collected 12.32 hours of Korean singing voices, including the voice of four singers and seven emotional intensity levels: neutral, and three levels

The authors are with Computer Science and Electrical Engineering Department, Handong Global University, Pohang 37554, Korea. (e-mail: sjkim@handong.ac.kr; 21800132@handong.ac.kr; junfa0118@handong.ac.kr; ijkim@handong.ac.kr)

each of happiness and sadness. In MOS tests and quantitative evaluations, Muse-SVS exhibited improved voice quality, expressiveness, and synchronization performance compared to baseline models. Furthermore, the visualization results presented in Section IV-F suggest that Muse-SVS learns attribute embeddings highly correlated to singer ID and emotional intensity and also suggest that Muse-SVS is able to express emotions by controlling subtle changes in pitch, energy, and phoneme duration. The audio samples are available online ¹.

Our main contributions include: 1) the first neural multi-singer emotional SVS that expresses emotional type and intensity, 2) per-attribute residual encoders for expressive SVS that adds variance to phoneme embeddings while minimizing interference between interdependent and overlapping attributes, 3) statistical pitch predictor predicting pitch variance according to emotional intensity while reliably following the note pitch sequence, 4) context-aware residual duration predictor that prevents the accumulation of variances in phoneme duration for accurate synchronization with the score, 5) emotion embedding interpolation and extrapolation to learn a continuous emotional space, thereby expressing emotional intensities not included in the training data, and 6) ASPP-Transformer to incorporate broad contexts while focusing on local details of singing voices with minimal increase in computation and parameters.

II. RELATED WORK

A. Single-singer SVS

The SVS models developed in the early days of deep learning have similar structures to conventional SVS systems, but some modules have been replaced with deep neural networks [27]. [4] proposed an end-to-end neural SVS model composed of an encoder and an attention-based autoregressive decoder. In addition, they improved voice quality by applying adversarial loss in training. Regarding speech synthesis, [28] proposed a non-autoregressive TTS model, FastSpeech, that resolves the skipping and repeating issues in autoregressive models. Inspired by FastSpeech, many SVS models have adopted the non-autoregressive architecture based on the feed-forward Transformer (FFT) [5], [6]. They are composed of an encoder that extracts high-level embeddings from the lyrics, note pitch, and note duration, a length regulator that aligns a sequence of phoneme embeddings to the spectrogram frames, and a decoder that synthesizes spectrograms from the aligned phoneme embeddings. In addition, some SVS models are based on GAN [29]–[31] and diffusion model [8].

B. Multi-Singer SVS

In the speech synthesis field, many multi-speaker TTS models reflect speaker ID by feeding a fixed-size speaker embedding into the decoder [32], [33]. Most multi-singer SVS models represent singer characteristics in similar ways [29], [34], [35]. However, learning the characteristics of multiple singers requires sufficient data for each singer. A few studies have learned singers’ characteristics from a small number of

samples. [36] learned the characteristics of each singer by adapting a pre-trained SVS model to the target singer. [34], [35], [37] presented zero-shot style adaptation methods that apply a reference encoder to extract singer embeddings from reference audio samples. In particular, [35] and [37] predicted frame-level singer embedding to capture time-varying singer characteristics by using an attention mechanism. Additionally, [35] applied multiple reference encoders to capture sufficient timbre information from multiple reference audio samples, while [37] proposed a local style token module to control musical expression not specified in the music score.

C. Emotion modeling in SVS

Most previous studies on emotional expression in SVS are based on traditional approaches. [21] analyzed the effect of F0 variances on emotional expression in singing voices, and proposed an F0 control module to reflect four types of F0 dynamics characteristics: overshoot, vibrato, preparation, and fine fluctuation. [10] proposed an SVS system based on hidden semi-Markov models (HSMM) that controls acoustic parameters affecting emotional expression. [22], [23] analyzed the effect of F0 variance, amplitude envelope, and spectral sequence on emotional expression. [24], [38] reported that variations in F0 and duration significantly affects recognized emotion. In TTS, many prior studies have controlled emotion through emotion embeddings [39]. However, to the best of our knowledge, there is no prior end-to-end neural SVS model that controls the type and intensity of emotion [11].

D. Multiple style modeling in unified embedding space

Many previous studies have represented style attributes in separate embedding spaces, implicitly assuming that style attributes are independent [40], [41]. However, since style attributes are correlated in reality, controlling an attribute without considering its effect on other attributes can cause interference. This problem is particularly serious for the multi-singer emotional SVS that controls many attributes while following the note pitch and note duration. To minimize interference, previous studies decorrelate attribute embeddings by gradient reversal [42], [43] or represent the relation between attributes by hierarchical embeddings [44]–[46]. However, they are insufficient for style attributes that are inherently correlated in a non-hierarchical way. [47] addressed this challenge by learning multiple attributes and their relations together in a unified embedding space as illustrated in Fig. 1.

We applied the idea of [47] with modifications to fit SVS. Muse-SVS avoids interference between attributes by representing all attributes and their relations by a joint embedding $E(y_i, z_1, \dots, z_N)$ in a unified embedding space, where y_i is the i -th phoneme and z_k denotes the k -th attribute. As shown in Fig. 1, Muse-SVS estimates the joint embedding by predicting the residual embedding $R(z_k|y_i, z_1, \dots, z_{k-1})$ of each attribute z_k conditional on the previous attributes z_1, \dots, z_{k-1} , and then combining them with the initial phoneme embedding $E(y_i)$ as

$$\begin{aligned} E(y_i, z_1, \dots, z_k) &= E(y_i, z_{<k}) + R(z_k|y_i, z_{<k}) \\ &= E(y_i) + \sum_{j=1}^k R(z_j|y_i, z_{<j}). \end{aligned} \quad (1)$$

¹<https://muse-svs.github.io/>

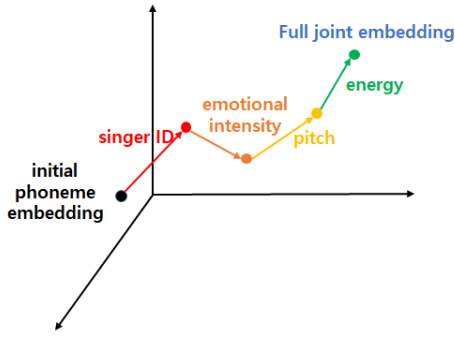


Fig. 1: The representation of multiple attributes by residual attribute embeddings in the unified embedding space. The coordinate of each point represents a joint embedding $E(y_i, z_{\leq k})$ of a phoneme y_k combined with zero or more attributes, z_1, \dots, z_k . The arrows represent the residual attribute embeddings $R(z_k|y_i, z_{<k})$ conditional on the previous attributes. The final coordinate corresponds to the full joint embedding $E(y_i, z_1, \dots, z_N)$ that represents all style attributes and their relations combined with the phoneme.

III. MUSE-SVS

A. Overall Architecture

Fig. 2a illustrates the structure of Muse-SVS. It takes lyrics (phoneme sequence), note pitch, and note duration as input. First, it converts the phonemes, note pitch, and note duration into embeddings using embedding tables. We concatenate the phoneme, pitch, and duration embeddings and apply a linear layer, in contrast to previous models [5] [6] that combine the embeddings by element-wise addition. The linear layer is a more general form than element-wise addition and exhibited higher fidelity in our preliminary experiments. Then, we add positional encoding [26] to the combined low-level embeddings. The encoder consists of FFT blocks and outputs the high-level representation of each phoneme combined with its pitch and duration information, which we call initial phoneme embedding and denote as $E(y_i)$.

The variance adaptor adds variance information to the initial phoneme embedding $E(y_i)$ according to style attributes z_k to build the full joint embedding $E(y_i, z_1, \dots, z_N)$, as shown in Fig. 2b. The variance adaptor consists of a collection of per-attribute predictors and encoders. Each attribute predictor predicts the value of the corresponding attribute, such as pitch and energy, while the attribute encoder produces the residual embedding $R(z_k|y_i, z_{<k})$ of the attribute. The variance adaptor adds the residual embeddings of style attributes z_1, \dots, z_N to the phoneme embedding sequentially, where z_1, \dots, z_4 are singer ID, emotional intensity, pitch, and energy, respectively. While the variance adaptor adds attributes to the phoneme, the embedding moves along the path $E(y_i), E(y_i, z_1), E(y_i, z_1, z_2), \dots, E(y_i, z_1, \dots, z_N)$, where $E(y_i, z_{\leq k}) = E(y_i, z_{<k}) + R(z_k|y_i, z_{<k})$ is a joint embedding that represents the phoneme y_i combined with attributes z_1, \dots, z_k . In Fig. 2b, the vertical arrows correspond to the joint embeddings $E(y_i, z_{\leq k})$ accumulating the residual attribute embeddings $R(z_k|y_i, z_{<k})$ for $1 \leq k \leq 4$.

Muse-SVS learns the residual attribute embeddings with residual attribute encoders $\hat{R}_k(\cdot)$ that take as input the previous

joint embeddings $E(y_i, z_{<k})$ to reflect the phoneme and the previous attributes. In Fig. 2b, the horizontal arrows from the vertical arrows represent the joint embeddings transmitted to the attribute predictors and encoders. Additionally, the singer and emotion encoders take as input attribute embeddings $E(z_k)$ retrieved from singer and emotion embedding tables, respectively. The embedding table learns the mean embedding of attribute z_k , in which the influence of the previous attribute was removed by normalization [47], [48]. The residual encoder $\hat{R}_k(E(z_k), E(y_i, z_{<k}))$ estimates the shift from $E(z_k)$ for adapting to the phoneme y_i and for reflecting the influence of the previous attributes. Therefore, the singer and emotion encoders have the form $\hat{R}_k(E(y_i, z_{<k}), E(z_k))$. The residual singer and emotion embedding tables were learned through knowledge distillation from a style encoder that is based on the global style token (GST) [14]. For more details, refer to [47].

On the other hand, the pitch (z_3) and energy (z_4) encoders take as input the output of the corresponding predictor, as $\hat{R}_k(E(y_i, z_{<k}), Pred_k(E(y_i, z_{<k})))$, where $Pred_k(\cdot)$ is either the pitch predictor $Pred_p(\cdot)$ or the energy predictor $Pred_e(\cdot)$. As the pitch and energy predictors refer to the previous attributes through the joint embedding $E(y_i, z_{<k})$, they predict pitch and energy differently according to emotional intensity, as shown in Fig. 9 and Fig. 11.

The duration predictor predicts the duration of each phoneme. We use $E(y_i, z_1, z_2)$ as its input because the duration can be affected by z_1 (singer ID) and z_2 (emotion), but independent of z_3 (pitch) and z_4 (energy). Consequently, it predicts phoneme durations differently according to emotional intensity, as shown in Fig.10. The length regulator aligns the sequence of joint embeddings $E(y_i, z_{1,\dots,4})$ to Mel-frames by duplicating the joint embeddings for the duration of each phoneme, similar to [49]. The decoder converts the aligned joint embeddings into a Mel-spectrogram. We also added a discriminator to improve fidelity through adversarial loss, similar to [4], [6], [7].

B. Statistical Pitch Predictor

SVS synthesizes a singing voice that follows the note pitch sequence. In addition to the macroscopic trend that matches the note pitch sequence, the emotional SVS should generate microscopic changes within the interval of each note because emotional intensities are often expressed by subtle pitch changes such as vibrato. SVS models without emotion modeling produce F0 sequences as close to the training samples as possible at the frame level without separating the two types of pitch changes [5], [6], [9], [50]. However, such an approach is sub-optimal for the emotional SVS because of a few reasons. First, estimating exact F0 trajectories is difficult because minute changes in the F0 are influenced by many situational factors [50] and are not sufficiently consistent. Second, to express emotion, it is not necessary to reproduce the F0 trajectory perfectly, including the phase of microscopic fluctuation, and imitating local pitch variance is sufficient. Third, the emotional SVS should control local pitch variation while keeping the macroscopic trend close to the

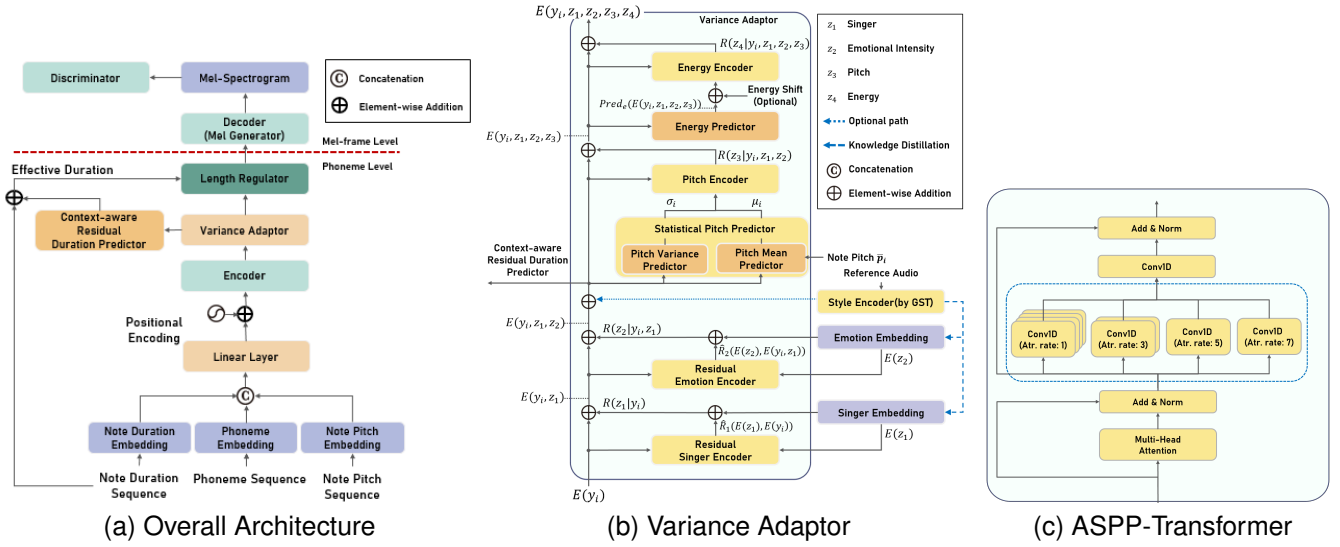


Fig. 2: The architecture of MuSE-SVS.

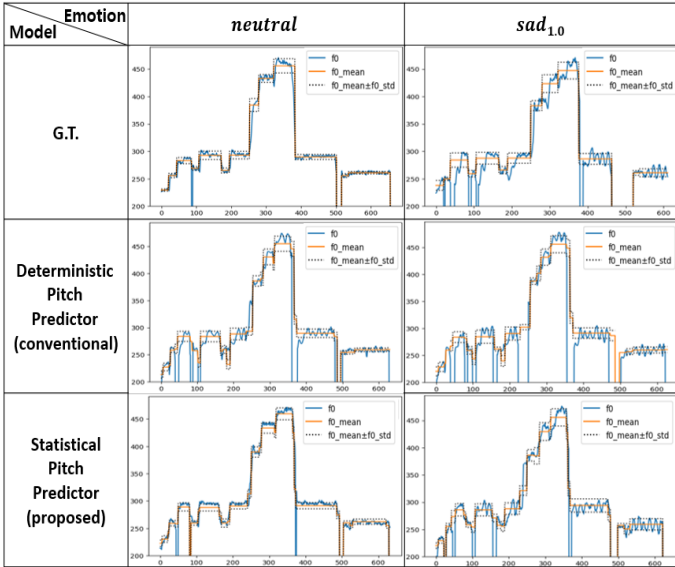


Fig. 3: The F0 contours (blue solid line) of a female singer’s voices with emotional intensity levels *neutral* (left) and *sad_{1.0}* (right). Each row displays the F0 contour of the ground truth samples (top), the output of Muse-SVS with the conventional deterministic pitch predictor (middle), and the output of Muse-SVS with the proposed statistical pitch predictor (bottom). The orange lines denote the mean of the F0 frequencies within the interval of each phoneme, and the black dotted lines denote the trajectory of mean±stdev. The deterministic pitch predictor produced vibrato with similar strengths regardless of emotional intensity. However, the proposed statistical pitch predictor produced vibrato of different strengths depending on emotional intensity while maintaining the macroscopic trend close to the note pitch sequence.

note pitch sequence. Therefore, we propose a novel statistical pitch predictor that estimates local pitch variances according to emotional intensity while reliably generating macroscopic pitch trends.

The proposed statistical pitch predictor estimates the distribution of the F0 frequencies at the phoneme level. The pitch predictor consists of a pitch mean predictor and a pitch variance predictor, and it estimates the local mean μ_i and local variance σ_i^2 of the F0 frequencies within the interval of each phoneme y_i . Both predictors take as input the joint embedding $E(y_i, z_1, z_2)$ to reflect the influence of singer ID (z_1) and emotional intensity (z_2). To reliably estimate mean pitch, the pitch mean predictor $Pred_{pm}(\cdot)$ estimates mean pitch $\hat{\mu}_i$ indirectly by first predicting the residual \hat{r}_i between the note pitch \hat{p}_i and the ground truth mean pitch μ_i measured from a training sample and then adding the predicted residual to the note pitch as $\hat{\mu}_i = \hat{p}_i + \hat{r}_i$. Previous studies have shown that such a residual pitch predictor helps mitigate the off-pitch problem [5], [50]. The pitch variance predictor $Pred_{pcv}(\cdot)$ predicts the coefficient of variation $CV_i = \sigma_i/\mu_i$ instead of σ_i^2 because pitch variances tend to be correlated with pitch means, whereas in CV_i , the correlation with pitch means is removed by normalization, making CV_i more reliably predictable [24]. During training, we optimize $Pred_{pm}(\cdot)$ and $Pred_{pcv}(\cdot)$ by the loss function presented in Eq. 2, where μ_i and CV_i are the ground truth mean pitch and pitch CV of phoneme y_i and \hat{CV}_i is the estimation of CV_i predicted by $Pred_{pcv}(\cdot)$. N_{pho} denotes the total number of phonemes. We set $\lambda_{pm} = 1$ and $\lambda_{pcv} = 10$.

$$\mathcal{L}_p = \lambda_{pm} \frac{1}{N_{pho}} \sum_i \sqrt{((\hat{p}_i + \hat{r}_i) - \mu_i)^2} + \lambda_{pcv} \frac{1}{N_{pho}} \sum_i \sqrt{(\hat{CV}_i - CV_i)^2} \quad (2)$$

Fig. 3 demonstrates the effectiveness of the proposed statistical pitch predictor. It displays the F0 contours of singing voices of the ground truth samples, the samples synthesized with the conventional deterministic pitch predictor, and the samples synthesized with the proposed statistical pitch predictor. In each F0 contour, the macroscopic trend follows the

note pitch sequence, while the microscopic changes exhibit singing techniques to express emotions, such as vibrato and bending. In the ground truth samples, the strength of vibrato increases with emotional intensity. The deterministic pitch predictor estimated major trends similar to the note pitch sequences but failed to generate differences in microscopic variances according to emotional intensity. By contrast, the proposed statistical pitch predictor produced vibrato of different strengths depending on emotional intensity while maintaining the macroscopic trend close to the note pitch sequence. The results of an ablation study, shown in Table IV, also show that the statistic pitch predictor significantly improves the expressiveness of Muse-SVS.

C. Context-aware Residual Duration Predictor (CRDP)

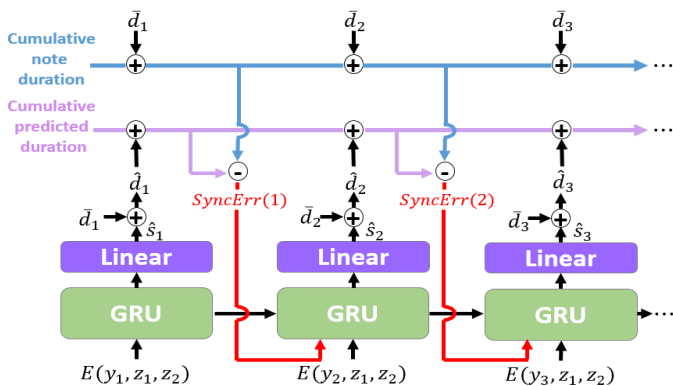


Fig. 4: The architecture of context-aware duration predictor

Synchronization with the music score is one of the fundamental requirements in SVS. A major source of synchronization error is the difference in cumulative duration between the synthesized voice and the music score. However, for an emotional SVS, it is not straightforward to maintain synchronization. In the singing voice, emotions are often expressed by subtle variances in phoneme duration, and the emotional SVS should imitate such variances. Naively minimizing the difference between the predicted and note durations at the phoneme level can suppress intentional variances for emotional expression, thereby resulting in loss of expressiveness. However, the accumulation of such variances impairs the tempo of the synthesized singing voice, making it difficult to play with musical instruments. This issue is particularly significant when synthesizing a long singing voice. Consequently, the emotional SVS should synthesize subtle variations in the duration of individual phonemes while suppressing synchronization errors due to the accumulation of such variations.

In conventional SVS models, the duration predictor predicts the duration of all phonemes in one step with a parallel architecture [5], [6], [9]. However, it is hard to prevent the accumulation of phoneme-level variances with such parallel predictors because they predict the duration of each phoneme independently without considering contexts. To address this problem, we propose a novel context-aware duration predictor (CRDP) that minimizes synchronization errors by considering

cumulative duration up to the previous phoneme when predicting the next phoneme duration while imitating variances in training samples to express emotions for individual phonemes. CRDP predicts the duration of phonemes sequentially with an autoregressive structure, as shown in Fig. 4. In predicting the duration of a phoneme, it takes the synchronization error of the previous phoneme and predicts the next phoneme duration inclined to compensate for the synchronization error.

At each step, CRDP takes as input the joint embedding $E(y_i, z_1, z_2)$ to reflect the influence of singer ID and emotional intensity. CRDP also takes the synchronization error of the previous step $SyncErr(i-1) = \sum_{j=1}^{i-1} \hat{d}_j - \sum_{j=1}^{i-1} \bar{d}_j$ as input, where \hat{d}_j and \bar{d}_j denote the predicted and note durations of a phoneme y_j , respectively. Similar to the pitch mean predictor, CRDP learns to estimate residual duration $s_i = d_i - \bar{d}_i$ as $\hat{s}_i = Pred_{d(i)}(E(y_i, z_1, z_2), SyncErr(i-1))$, where d_i denotes the ground truth phoneme duration measured from the training sample. Then, CRDP adds the predicted residual to the note duration as $\hat{d}_i = \bar{d}_i + \hat{s}_i$.

It is noteworthy that the emotional SVS should learn from both the ground truth duration and the note duration. While the former is to learn emotional expression, the latter is to learn synchronization with the music score. During training, we optimize $Pred_{d(i)}(\cdot)$ using the duration loss presented in Eq. 3. The first term draws the predicted duration of the individual phoneme close to the ground truth duration, thereby leading the predictor to imitate the subtle variation in training samples to express emotions. The second term leads the predictor to learn to compensate for the synchronization error between cumulative predicted duration and cumulative note duration. Eq. 3 does not penalize the difference between the predicted and note durations for individual phonemes but does penalize the difference in their accumulations. Consequently, CRDP maintains synchronization with the score without loss of expressiveness. In our experiments, we set $\lambda_{SyncErr} = 0.3$.

$$\mathcal{L}_d = \frac{1}{N_{pho}} \left[\sum_i (\hat{d}_i - d_i)^2 + \lambda_{SyncErr} \cdot \left| \sum_i SyncErr(i) \right| \right] \quad (3)$$

Fig. 5 displays the duration and pitch sequence of a 67.07-second long song and the singing voices synthesized with CRDP and two baseline duration predictors. The first baseline predictor (3rd row) applies note normalization introduced by VISinger [9], while the second baseline predictor (4th row) applies syllable duration loss used in XiaoiceSing [5]. The lengths of the audio samples are 67.07, 67.08, 60.11, and 62.24 seconds, respectively. The note-level MAE of the three models were merely 0.064, 0.075, and 0.080 seconds, implying that all three predictors reasonably estimate the duration of individual phonemes. However, the baseline models exhibited significant synchronization errors of 6.69 and 4.83 seconds at the end of the song, suggesting that minimizing prediction errors for individual phonemes is insufficient to prevent the accumulation of variances in phoneme duration. By contrast, the synchronization error of CRDP was 0.01 seconds, which is significantly lower than those of the baseline predictors.

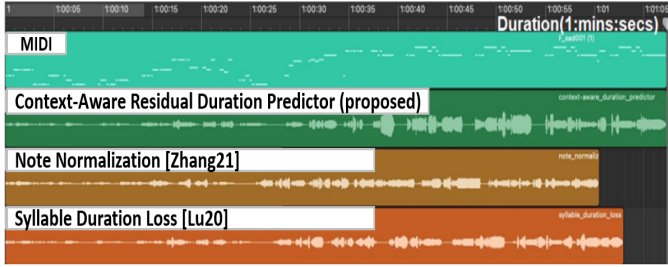


Fig. 5: The synchronization errors of duration predictors for a long song composed of 117 notes whose length is 67.08 seconds. 1st row: the duration and pitch sequence of a song in MIDI format. 2nd-4th rows: singing voices synthesized with CRDP (proposed) and two baseline predictors applying note normalization [9] and syllable duration loss [5], respectively. The note-level MAE of the three models are 0.064, 0.075, and 0.080 seconds from the top. However, their synchronization errors at the end of the song are 0.01, 6.96, and 4.83 seconds. CRDP exhibited a significantly lower synchronization error than the baseline predictors for a long song.

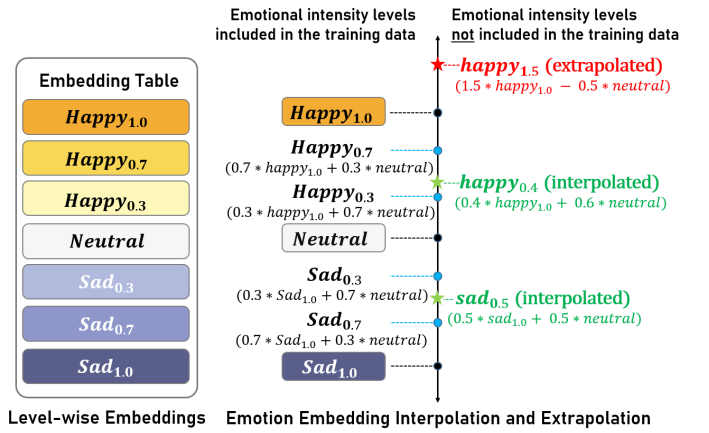
We also conducted a quantitative evaluation of synchronization performance and presented the result in Table VI.

D. Emotion Embedding Interpolation and Extrapolation

Previous studies have reflected emotions in voices by feeding emotion embeddings to the model [18], [42], [47], [51]. As described in III-A, Muse-SVS predicts residual emotion embeddings by combining an embedding table and a residual encoder as $R(z_2|y_i, z_1) = E_2(z_2) + \hat{R}_2(E_2(z_2), E(y_i, z_1))$. For simplicity, we denote the residual embedding for an emotional intensity level v as $r_v = R(v|y_i, z_1)$.

We considered two methods to learn the embeddings of multiple emotional intensity levels: level-wise embeddings, and embedding interpolation. The former learns separate embeddings for each emotional intensity level, while the latter learns only one embedding for each emotional type and represents intensity levels by embedding interpolation, as shown in Fig. 6. Our training data contains seven emotional intensity levels: $happy_{1.0}$, $happy_{0.7}$, $happy_{0.3}$, $neutral$, $sad_{0.3}$, $sad_{0.7}$, and $sad_{1.0}$. Therefore, Muse-SVS learns seven separate embeddings with the level-wise embedding table. However, with emotion interpolation, it learns only three embeddings, each of which is for $happy_{1.0}$, $neutral$, and $sad_{1.0}$, and computes the embeddings of intermediate intensity levels by interpolation as $r_{happy_t} = t \cdot r_{happy_{1.0}} + (1 - t) \cdot r_{neutral}$ and $r_{sad_t} = t \cdot r_{sad_{1.0}} + (1 - t) \cdot r_{neutral}$. A prior study [18] also applies emotion interpolation to mix different types of emotion. However, they only apply embedding interpolation to synthesis, whereas we apply it to both training and synthesis.

Muse-SVS applies emotion embedding interpolation because it has multiple advantages over level-wise emotion embeddings. First, it is possible to express intermediate intensity levels, such as $happy_{0.5}$ and $sad_{0.8}$, that are not in the training data. Second, it enables the synthesis of singing voices with emotional intensities beyond those in the training data by emotion embedding extrapolation with $t > 1$. Our demo page



Level-wise Embeddings Emotion Embedding Interpolation and Extrapolation

Fig. 6: The representation of emotional intensity levels by level-wise embeddings (left) and embedding interpolation (right). Muse-SVS can express emotional intensities that are not in the training data through emotion embedding interpolation and extrapolation.

presents audio samples produced by emotion embedding extrapolation. Third, applying emotion embedding interpolation during training causes the model to reflect the neighborhood relation between emotional intensity levels, thereby learning a linear embedding space, as shown in Fig. 8b.

E. ASPP-Transformer

The variations in phoneme duration in the singing voice is substantially higher than that of ordinary voices. To synthesize high-fidelity singing voices, the receptive field of the decoder should be sufficiently large because the decoder processes high-resolution feature maps at the frame level. Meanwhile, to effectively learn fine-grained acoustic features, which are important for expressing emotion [24], the decoder should catch local details as well. Each FFT block consists of a multi-head self-attention (MSA) sublayer and a feed-forward sublayer composed of two convolution operators.

Previous studies have shown that convolution refers to a limited context [52]–[54]. Although the MSA sublayer refers to broader contexts than convolution, enhancing the receptive field of convolution is essential because convolution plays an important role in Muse-SVS. In the preliminary experiments, we observed that the average activation of the feed-forward sublayers was twice higher than that of the MSA sublayers, suggesting that the contribution of convolution can be greater than MSA. However, simply enlarging convolution filters drastically increases computational cost and the number of parameters, thereby increasing the risk of overfitting.

To overcome this challenge, we extended FFT by replacing convolution with atrous spatial pyramid pooling (ASPP) [25], as shown in Fig. 2c. This new building block is called ASPP-Transformer. ASPP-Transformer inherits the advantage of ASPP in that it can refer to a broad context, with minimal increase in computation and parameters. Focusing on the local neighborhoods while incorporating a broad context, we assigned a large number of channels to the filters with low atrous rates.

Fig. 7 compares the effective receptive fields of the decoders composed of the proposed ASPP-Transformer and ordinary Transformer blocks. The first row displays the gradient norm of an output node with respect to the input embeddings aligned to the frame-level resolution by the length regulator. The gradient norm measures the importance of the input on the output [55]. The right column shows that the ordinary Transformer has a limited effective receptive field, leading to discontinuous Mel-spectrogram and unstable vibrato. In contrast, ASPP-Transformer refers to broader contexts than ordinary Transformer, producing a more stable Mel-spectrogram and vibrato, thereby leading to improved fidelity and expressiveness.

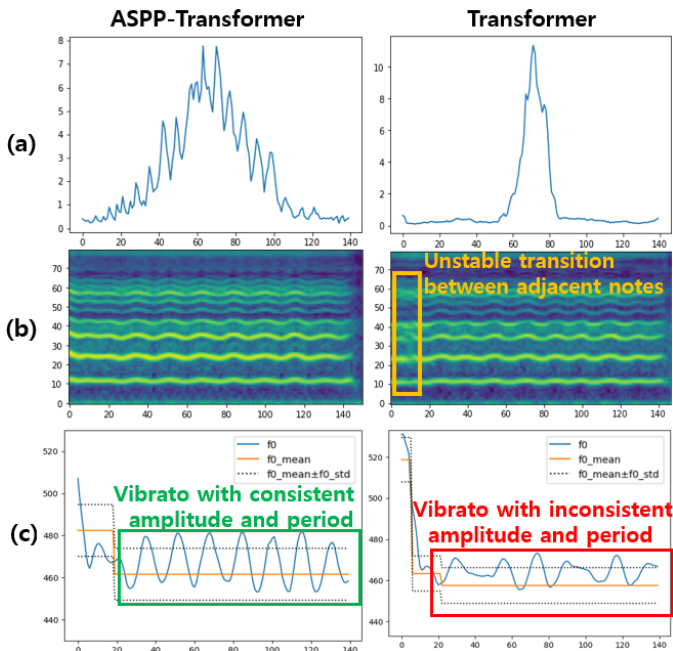


Fig. 7: The effective receptive fields and output of the decoders composed of the proposed ASPP-Transformer and ordinary Transformer. The first row displays the L_1 norm of the gradient of the 70th output node with respect to the input embeddings aligned to frame-level resolution ($\frac{\partial x_{70}}{\partial E(y_{j,z_{1:4}})}, 1 \leq j \leq 140$). The second and third rows display the synthesized Mel-spectrograms and their F0 contours, respectively.

F. Training of Muse-SVS

We train Muse-SVS by minimizing the L_1 reconstruction loss \mathcal{L}_m between the ground truth and the synthesized Mel-spectrograms. The synthesized Mel-spectrogram often has a different length from the ground truth Mel-spectrogram. Therefore, we apply soft dynamic time warping [56] to align the two Mel-spectrograms. We also minimize the L_2 reconstruction loss between the predicted pitch, energy, and duration, and those of the training sample to improve the accuracy of the predictors. In addition, we combine an adversarial loss \mathcal{L}_{adv} to alleviate the over-smoothing issue, following [4], [6], [7]. The total loss \mathcal{L}_{total} combines those losses by weighted sum as Eq. 4, where \mathcal{L}_p , \mathcal{L}_e , and \mathcal{L}_d are the L_2 losses for pitch, energy, and duration, respectively. λ_m , λ_p , λ_e , λ_d , and λ_{adv} denote the weights of the losses. In experiments, we set

$\lambda_m, \lambda_p, \lambda_e, \lambda_d$ to 1, 1, 0.8, 0.8. We initially set λ_{adv} to 0.01 to warm up and then gradually increase to 0.5.

$$\mathcal{L}_{total} = \lambda_m \mathcal{L}_m + \lambda_p \mathcal{L}_p + \lambda_e \mathcal{L}_e + \lambda_d \mathcal{L}_d + \lambda_{adv} \mathcal{L}_{adv} \quad (4)$$

G. Data collection

To collect a singing voice dataset, we selected 69 Korean pop songs and categorized them into happy and sad songs. Subsequently, four singers (two male and two female) sang the selected songs four times at different emotional intensity levels: *happy*_{1.0}, *happy*_{0.7}, *happy*_{0.3}, and *neutral* for the happy songs, and *sad*_{1.0}, *sad*_{0.7}, *sad*_{0.3}, and *neutral* for the sad songs. Two of the singers are professionals, while the other two are amateurs with good singing skills.

The biggest challenges were setting singing guidelines for each emotional intensity level and leading the singers to follow the guidelines while singing. We consulted a vocal trainer to set the singing guidelines for each emotional intensity level. The singing guidelines consist of vocalization methods, the ratio of respiration and resonance, and singing techniques to express each emotional intensity level. Afterward, the professional singers sang the songs at each emotional intensity level according to the guidelines. We collected one hour of reference singing voice samples from the two professional singers. With the singing guidelines and the reference singing voices, we guided the amateur singers to sing at different emotional intensity levels. In this way, we collected additional 11.23 hours of singing voice samples from the two amateur singers.

IV. EXPERIMENTS

A. Dataset

For experiments, we combined our dataset described in the previous section and 2.12 hours of Korean singing voices in the Children’s Song Dataset (CSD) [57]. The combined dataset consists of 7,672 singing voice samples that are 5-10 seconds long, sung by five singers. Of the total samples, we used 7,120 for training and 552 samples for testing. Since the samples in the CSD dataset do not have emotion labels, we labeled all of them as *neutral*.

B. Details of SVS models

1) **Muse-SVS**: Muse-SVS consists of multiple modules, as shown in Fig. 2a. The encoder consists of six FFT blocks. The variance adaptor (VA) consists of per-attribute predictors and per-attribute encoders. The context-aware residual duration predictor consists of a gated recurrent unit (GRU) and a linear layer. The decoder consists of six ASPP-Transformer blocks. We built the discriminator based on SF-GAN [6] and the reference encoder based on the global style tokens (GST) [14]. The hyperparameters of the modules are presented in Table I.

TABLE I: The hyperparameters of Muse-SVS

NETWORK	HYPERPARAMETER	
PHONEME EMBEDDING DIMENSION		384
ENCODER	LAYERS	6
	MSA HEADS	2
	MSA HIDDEN DIM.	384
	1ST CONV1D KERNEL SIZE	9
	1ST CONV1D FILTERS	1536
	2ND CONV1D KERNEL SIZE	1
	2ND CONV1D FILTERS	384
	DROPOUT RATE	0.2
DECODER	LAYERS	6
	MSA HEADS	2
	MSA HIDDEN DIM.	384
	ASPP KERNEL SIZE	9
	ASPP KERNEL DILATION RATE	[1, 3, 5, 7]
	ASPP FILTERS	[768, 384, 192, 192]
	CONV1D KERNEL SIZE	1
	CONV1D FILTERS	384
PER-ATTRIBUTE PREDICTORS OF VA	LAYERS	2
	CONV1D KERNEL	3
	CONV1D FILTER SIZE	384
	DROPOUT RATE	0.5
PER-ATTRIBUTE ENCODERS OF VA	CONV1D KERNEL	3
	CONV1D FILTER SIZE	384
	DROPOUT RATE	0.5
CONTEXT-AWARE RESIDUAL DURATION PREDICTOR	HIDDEN DIM	384
REFERENCE ENCODER	LAYERS	6
	CONV2D KERNEL	(3, 3)
	CONV2D FILTER SIZE	(32, 32, 64, 64, 128, 128)
	CONV2D STRIDE	(2, 2)
	HIDDEN DIM OF GRU	192
STYLE TOKEN LAYER	TOKENS	10
	TOKEN DIM.	48
	ATTENTION HIDDEN DIM.	384
	ATTENTION HEADS	8
DISCRIMINATOR	LAYERS	3
	CONV2D KERNEL	(9, 9)
	CONV2D FILTER SIZE	(1, 64, 64, 64, 64, 64)
	CONV2D STRIDE	(1, 1)
TOTAL NUMBER OF PARAMETERS		101M

2) **Baseline models for comparison:** We built two multi-singer emotional SVS models to compare with Muse-SVS by extending FastSpeech2 [49] and VISinger [9].² These are referred to as MSME-FFTSinger and MSME-VISinger. The structure of MSME-FFTSinger differs from FastSpeech2 in three aspects: 1) The encoder was extended to take as input the combined embedding of the phoneme, note pitch, and note duration to synthesize singing voices. 2) To reflect singer ID and emotion, MSME-FFTSinger retrieves the singer and emotion embeddings from embedding tables and adds them to the combined phoneme embedding. 3) MSME-FFTSinger predicts pitch and energy at the phoneme level, while FastSpeech2 predicts them at the frame level. This modification improved stability in our preliminary experiments.

To build MSME-VISinger, we first reproduced VISinger from the open-source of its baseline model, VITS [58]³, because we could not find a publicly available implementation of VISinger. Subsequently, we extended it to a multi-singer emotional SVS by applying the techniques introduced in [58]. We extended the residual blocks of the posterior encoder and

the normalizing flow to be conditional on singer and emotion embeddings, and added singer and emotion embeddings to the input of the decoder.

3) **Models for ablation study:** We built three more SVS models derived from Muse-SVS for the ablation study. In the first model, Muse-SVS(w/o SPP), the statistical pitch predictor was replaced with the deterministic pitch predictor. In the second model, Muse-SVS(w/o ASPP), the ASPP-Transformer blocks were replaced with ordinary FFT blocks. Finally, the third model, Muse-SVS(uncond) does not apply the conditional attribute predictors and encoders, and estimates attribute embeddings unconditionally with embedding tables $E(z_k)$.

C. Training of the SVS models

Muse-SVS, MSME-FFTSinger, and the models for the ablation studies were trained for two days on a single RTX-3090 GPU with 24 GB memory. We used the ADAM optimizer with a learning rate of 0.001, $\beta_1=0.9$, $\beta_2=0.98$, $\epsilon=10^{-9}$, and batch size of 8. In addition, we followed the same learning rate schedule of [26]. We trained MSME-VISinger for 14 days on two RTX-3090 GPUs and a batch size of 8 for each GPU. MSME-VISinger was trained using the AdamW optimizer where the initial learning rate, β_1 , β_2 , weight decay λ were

²Since Muse-SVS is the first multi-singer emotional SVS model, there is no existing baseline model for comparison.

³<https://github.com/jaywalnut310/vits>

TABLE II: The results of MOS tests for voice quality and expressiveness

METHODS	VOICE QUALITY(↑)			EXPRESSIVENESS(↑)		
	PRONUNCIATION	SOUND	NATURALNESS	SINGER'S	EMOTIONAL	EMOTIONAL
	ACCURACY	QUALITY		TIMBRE	TYPE	INTENSITY
				SIMILARITY	SIMILARITY	SIMILARITY
G.T.	4.23±0.30	4.70±0.16	4.71±0.14	-	-	-
MSME-FFTSINGER	2.93±0.34	2.81±0.35	3.18±0.28	3.16±0.39	3.35±0.27	3.06±0.35
MSME-VISINGER	4.20±0.27	3.72±0.23	3.31±0.30	3.00±0.42	2.98±0.28	2.35±0.41
MUSE-SVS	4.31±0.28	4.45±0.17	4.41±0.20	3.98±0.33	4.38±0.19	4.07±0.30

TABLE III: The result of ablation studies for voice quality

METHODS	VOICE QUALITY	
	SOUND QUALITY	NATURALNESS
MUSE-SVS	0	0
MUSE-SVS(w/o SPP)	+0.03	-0.53
MUSE-SVS(w/o ASPP)	-0.28	-0.98
MUSE-SVS(UNCOND)	-0.49	-0.22

set to 2×10^{-4} , 0.8, 0.99, and 0.01, respectively. Furthermore, we decreased the learning rate by $0.999^{1/8}$ after every epoch.

D. Subjective evaluation by MOS tests

We evaluated the voice quality and expressiveness of the SVS models by MOS and CMOS tests with 30 subjects⁴. The subjects evaluated the voice quality of the synthesized voices in terms of pronunciation accuracy, sound quality, and naturalness. They also evaluated the expressiveness of the models by singer similarity, emotional type similarity, and emotional intensity similarity. To assess singer and emotional type similarities, we asked the subjects to compare the timbre and emotional type of the synthesized samples to those of the ground truth samples. Regarding the similarity in emotional intensity, the subjects first listened to a pair of ground truth samples sung with two different emotional intensity levels, and then listened to a pair of synthesized samples with the same emotional intensity levels as those of the ground truth samples. Finally, the subjects evaluated how close the gap in emotional intensities between the synthesized samples is to the gap between the ground truth samples.

1) **Evaluation of voice quality and expressiveness:** Table II summarizes the evaluation results of Muse-SVS and the baseline models. Muse-SVS exhibited the highest MOS in all metrics. MSME-VISinger showed the second-best results in the metrics for voice quality evaluation. However, in regard to expressiveness, MSME-FFTSinger exhibited higher MOS than MSME-VISinger.

2) **Ablation study:** To evaluate the effectiveness of the proposed methods, we conducted a CMOS test for sound quality and naturalness (Table III). Removing the statistical pitch variance predictor, as in Muse-SVS(w/o SPP), substantially decreased the naturalness score by -0.53, whereas the sound quality score was slightly increased by +0.03. This implies that the statistical modeling of the F0 frequencies

TABLE IV: The result of ablation studies for expressiveness

METHODS	EXPRESSIVENESS(↑)		
	SINGER'S	EMOTIONAL	EMOTIONAL
	TIMBRE	TYPE	INTENSITY
	SIMILARITY	SIMILARITY	SIMILARITY
MUSE-SVS	3.98±0.33	4.38±0.19	4.07±0.30
w/o ASPP	2.68±0.33	3.69±0.23	3.02±0.32
w/o SPP	3.02±0.43	3.88±0.27	2.98±0.43
UNCOND	3.22±0.52	3.57±0.32	3.56±0.35

helps synthesize a natural singing voice. When the ASPP-Transformer blocks were replaced by ordinary FFT blocks, as in Muse-SVS(w/o ASPP), the sound quality score decreased by -0.28 while the naturalness score decreased by -0.98. This suggests that ASPP-Transformer, which refers to broad contexts, is effective in improving voice quality, particularly in terms of naturalness. Muse-SVS(uncond) showed the sound quality score decreased by -0.49 and the naturalness score decreased by -0.22. These results suggest that predicting style attribute embeddings conditional on the previous attributes improves sound quality and naturalness.

Table IV presents the results of the ablation study for singer similarity, emotional type similarity, and emotional intensity similarity. Muse-SVS exhibited remarkably higher MOS scores than those of other models, suggesting that the proposed methods are effective in improving the expressiveness of the SVS model. Particularly, ASPP-Transformer and statistical pitch predictor significantly improved singer similarity and emotional intensity similarity.

E. Quantitative evaluation

1) **Pitch prediction:** The emotional SVS should effectively learn the emotions expressed in the training data, which are often conveyed by pitch variances. To evaluate how closely each SVS model imitates the pitch variances of the training data, we compared the phoneme-wise pitch distributions of the synthesized and ground truth samples by Fréchet distance [59] as in Eq. 5, where $F[\cdot]$, L_n , and N denote Fréchet distance, the number of phonemes in the n -th sample, and the number of samples, respectively. $N(\hat{\mu}_i, \hat{\sigma}_i^2)$, $N(\mu_i, \sigma_i^2)$ are Gaussian distributions parameterized by the mean and variance of the synthesized and ground truth pitch values in the interval of each phoneme, respectively.

$$Error_p = \frac{1}{N} \sum_{n=1}^N \sum_{i=1}^{L_n} F[N(\hat{\mu}_i, \hat{\sigma}_i^2), N(\mu_i, \sigma_i^2)] \quad (5)$$

⁴Many previous studies on TTS and SVS listed in our references present the result of MOS test evaluated by 10-20 subjects [5], [6], [28], [47], [49]

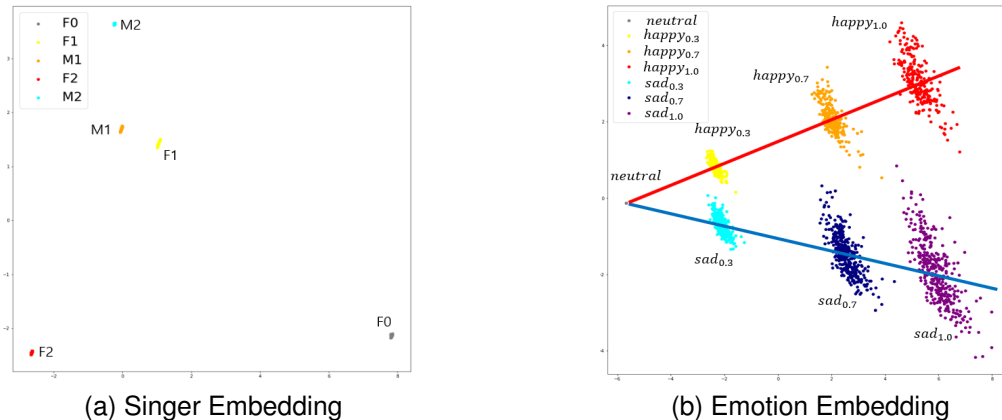


Fig. 8: The distribution of residual attribute embeddings visualized by PCA. left; residual singer embeddings $R(z_1|y_i)$ colored by singer label, right: residual emotion embeddings $R(z_2|y_i, z_1)$ colored by emotion label. The attribute embeddings are clustered according to their labels, which indicates that Muse-SVS learns attribute embeddings highly correlated with the corresponding attribute labels. We manually drew the lines in the right figure for the convenience of the reader.

TABLE V: Fréchet distance between pitch distributions (Eq. 5) in the synthesized and ground truth samples

METHODS	$Error_p(\downarrow)$
MUSE-SVS	148.82
MUSE-SVS(w/o SPP)	174.89
MSME-VISINGER	172.64

We compared three SVS models: MSME-VISinger, Muse-SVS(w/o SPP), and Muse-SVS. MSME-VISinger predicts F0 frequencies at the frame level, whereas the other two models predict F0 frequencies at the phoneme level. MSME-VISinger and Muse-SVS(w/o SPP) predict pitch deterministically, while Muse-SVS predicts statistically. Table V presents the evaluation results. The results show that MSME-VISinger and Muse-SVS(w/o SPP) exhibited comparable Fréchet distances. Muse-SVS exhibited significantly lower Fréchet distance compared with the two baseline models, indicating that the proposed statistical pitch predictor synthesizes pitch distributions close to those of the training data.

2) **Synchronization with note duration sequence:** To evaluate the effectiveness of the proposed CRDP in synchronization with the score, we measured synchronization error for the test samples using Eq. 6, where N , L_n , \hat{d}_i , and \bar{d}_i denote the number of samples, the number of phonemes in each sample, the predicted phoneme duration, and the note duration, respectively. Eq. 6 measures the synchronization error normalized by the total length of the song. In addition, we measured the RMSE between \hat{d}_i and ground truth phoneme duration d_i , as Eq. 7.

$$Error_s = \frac{1}{N} \sum \frac{1}{\sum_{i=1}^{L_n} \bar{d}_i} \left| \sum_{i=1}^{L_n} \hat{d}_i - \sum_{i=1}^{L_n} \bar{d}_i \right| \quad (6)$$

$$RMSE_d = \frac{1}{N} \sum \sqrt{\frac{1}{L_n} \sum_{i=1}^{L_n} (d_i - \hat{d}_i)^2} \quad (7)$$

TABLE VI: The synchronization and duration prediction performances of duration predictors. 2nd column: the average of synchronization errors at the end of each sample (Eq. 6). 3rd column: the RMSE of phoneme-level duration prediction in seconds and the number of frames (Eq. 7).

METHODS	$Error_s(\downarrow)$	$RMSE_d(\downarrow)$
NOTE NORMALIZATION [9]	4.7%	0.025 (2.33)
SYLLABLE DURATION LOSS [5]	6.6%	0.027 (2.51)
CRDP (PROPOSED)	0.2%	0.026 (2.44)

We compared the proposed CRDP with two baseline duration predictors that apply note normalization [9] and syllable duration loss [5], respectively. The first baseline predictor learns and predicts the ratio of the ground truth phoneme duration to the corresponding note duration, and then estimates phoneme duration by multiplying the corresponding note duration by the predicted ratio. The second baseline predictor was trained by a combination of phoneme-level and syllable-level duration losses [5], and it directly predicts phoneme duration.

Table VI presents the evaluation results. The two baseline predictors exhibited synchronization errors of 4.7% and 6.6%, respectively. By contrast, the proposed CRDP exhibited a remarkably lower synchronization error of 0.2%. Regarding phoneme-level duration prediction, the first baseline predictor exhibited the lowest RMSE, while the proposed CRDP exhibited showed the second lowest. However, the differences in phoneme-level RMSEs were insignificant. These results demonstrate that CRDP significantly improves synchronization performance while maintaining phoneme-level prediction accuracy.

F. Visualization analysis

1) **Visualization of embedding spaces:** Muse-SVS represents style attributes z_k by conditional residual embeddings $R(z_k|y_i, z_{\leq k})$ in a unified embedding space. We visualized the distribution of the residual embeddings using principal component analysis (PCA). Fig. 8 displays the distribution of

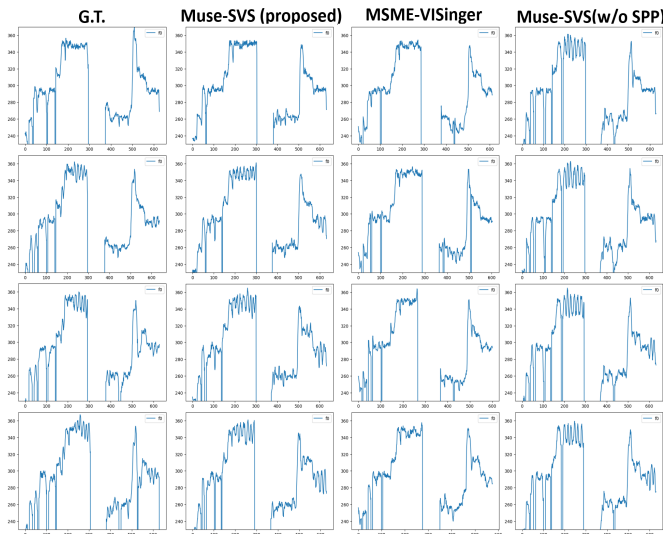


Fig. 9: The F0 contours of the singing voices synthesized with different emotional intensities. From the top, each row displays the pitch contours synthesized with emotional intensity levels *neutral*, *sad*_{0.3}, *sad*_{0.7}, and *sad*_{1.0}, respectively.

the residual singer and emotion embeddings colored by singer and emotion labels, respectively. The singer and emotion embeddings are clustered according to their labels, indicating that the proposed methods learn attribute embeddings that are highly correlated with the corresponding attribute labels. In particular, due to the embedding interpolation used in training, the embedding distributions of the emotional intensity levels are linearly aligned as shown in Fig. 8b.

2) **F0 contours varying with emotional intensity:** To analyze the effectiveness of the proposed statistical pitch predictor, we visualized the pitch contours synthesized by Muse-SVS and two baseline models, MSME-VISinger and Muse-SVS(w/o SPP), as depicted in Fig. 9. Muse-SVS controlled the strength of vibrato according to the emotional intensity, while MSME-VISinger failed to exhibit significant differences according to the emotional intensity. However, when the statistical pitch predictor was replaced by a deterministic pitch predictor, as in Muse-SVS(w/o SPP), the model was unable to control the strength of vibrato according to the emotional intensity anymore.

3) **Predicted durations varying with emotional intensity:** We visualized the Mel-spectrogram synthesized by Muse-SVS with different emotional intensity levels, as shown in Fig. 10. Muse-SVS predicted phoneme durations differently according to emotional intensity. Nevertheless, both Mel-spectrograms remain synchronized with the note pitch sequence until the end of the song.

4) **Energy contours varying with emotional intensity:** We visualized the energy contours of the synthesized samples to check whether Muse-SVS controls energy according to emotional intensity. Fig. 11 displays the energy contours synthesized by Muse-SVS, MSME-VISinger, and MSME-FFTSinger. In the ground truth samples, as the emotional intensity level changes from *neutral* to *sad*_{1.0}, the energy contour fluctuated more while the decrescendo and vibrato

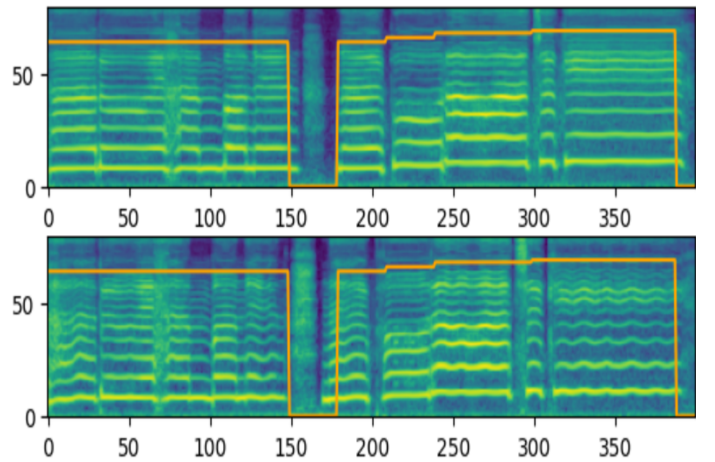


Fig. 10: Mel-Spectrograms synthesized by Muse-SVS with emotional intensity levels *neutral* (top) and *happy*_{1.0} (bottom). The orange lines denote the note pitch sequence. Muse-SVS predicted phoneme durations differently depending on emotional intensity while maintaining sync with the note pitch sequence until the end of the song.

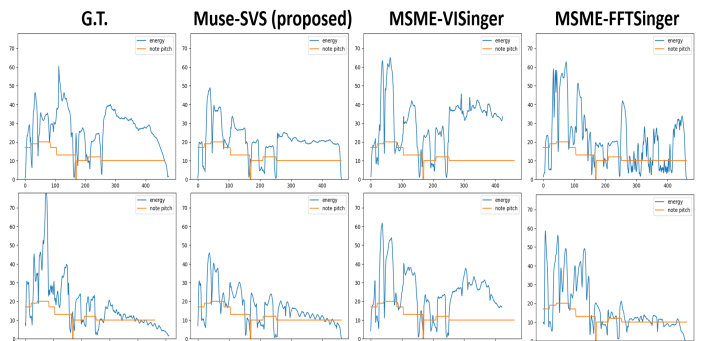


Fig. 11: The energy contours of the singing voices synthesized with *neutral* (top) and *sad*_{1.0} (bottom). With emotional intensity level *sad*_{1.0}, Muse-SVS produced more fluctuating energy contour and expressed decrescendo and vibrato.

become pronounced. Muse-SVS produced a similar change in energy contour, while the other models did not, as shown in Fig. 11.

V. CONCLUSION

In this study, we proposed Muse-SVS, the first multi-singer emotional singing voice synthesizer that expresses multiple levels of emotional intensities. Muse-SVS synthesizes singing voices from lyrics, note pitch, and note duration controlling multiple attributes such as singer ID and emotional intensity. It synthesizes subtle variations in pitch, energy, and phoneme duration according to emotional intensity while accurately synchronizing with the music score. To avoid interference between non-hierarchically correlated attributes, Muse-SVS represents multiple style attributes by a joint embedding in a unified embedding space that encodes all attributes and their relations together. We presented multiple novel techniques to improve the voice quality and expressiveness of SVS, including a statistical pitch predictor, context-aware

duration predictor, and ASPP-Transformer. Compared with the baseline models, Muse-SVS exhibited improved voice quality, expressiveness, and synchronization performance in MOS tests and quantitative evaluations. We also presented visualization results demonstrating that Muse-SVS learns attribute embeddings highly correlated with the corresponding attribute labels, and that Muse-SVS successfully controls subtle changes in pitch, energy, and phoneme duration according to emotions.

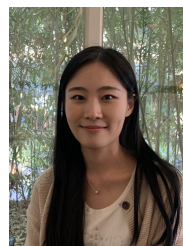
REFERENCES

- [1] M. Macon, L. Jensen-Link, E. B. George, J. Oliverio, and M. Clements, "Concatenation-based midi-to-singing voice synthesis," in *Audio Engineering Society Convention 103*. Audio Engineering Society, 1997.
- [2] K. Saino, H. Zen, Y. Nankaku, A. Lee, and K. Tokuda, "An hmm-based singing voice synthesis system," in *9th International Conference on Spoken Language Processing*, 2006.
- [3] H. Kenmochi and H. Ohshita, "Vocaloid-commercial singing synthesizer based on sample concatenation," in *Proceedings of the Annual Conference of the International Speech Communication Association (INTERSPEECH)*, vol. 2007, 2007, pp. 4010–4011.
- [4] J. Lee, H.-S. Choi, C.-B. Jeon, J. Koo, and K. Lee, "Adversarially trained end-to-end korean singing voice synthesis system," in *Proceedings of the Annual Conference of the International Speech Communication Association (INTERSPEECH)*, vol. 2019, 2019, pp. 2588–2592.
- [5] P. Lu, J. Wu, J. Luan, X. Tan, and L. Zhou, "Xiaoice-singer: A high-quality and integrated singing voice synthesis system," in *Proceedings of the Annual Conference of the International Speech Communication Association (INTERSPEECH)*, vol. 2020, 2020, pp. 1306–1310.
- [6] J. Chen, X. Tan, J. Luan, T. Qin, and T.-Y. Liu, "Hifisinger: Towards high-fidelity neural singing voice synthesis," *arXiv preprint arXiv:2009.01776*, 2020.
- [7] G.-H. Lee, T.-W. Kim, H. Bae, M.-J. Lee, Y.-I. Kim, and H.-Y. Cho, "N-Singer: A Non-Autoregressive Korean Singing Voice Synthesis System for Pronunciation Enhancement," in *Proceedings of the Annual Conference of the International Speech Communication Association (INTERSPEECH)*, vol. 2021, 2021, pp. 1589–1593.
- [8] J. Liu, C. Li, Y. Ren, F. Chen, and Z. Zhao, "DiffSinger: Singing voice synthesis via shallow diffusion mechanism," in *Proceedings of the AAAI Conference on Artificial Intelligence*, vol. 36, no. 10, 2022, pp. 11 020–11 028.
- [9] Y. Zhang, J. Cong, H. Xue, L. Xie, P. Zhu, and M. Bi, "Visinger: Variational inference with adversarial learning for end-to-end singing voice synthesis," in *ICASSP 2022-2022 IEEE International Conference on Acoustics, Speech and Signal Processing (ICASSP)*. IEEE, 2022, pp. 7237–7241.
- [10] Y. Park, S. Yun, and C. D. Yoo, "Parametric emotional singing voice synthesis," in *ICASSP 2010 IEEE International Conference on Acoustics, Speech and Signal Processing (ICASSP)*. IEEE, 2010, pp. 4814–4817.
- [11] Y.-P. Cho, F.-R. Yang, Y.-C. Chang, C.-T. Cheng, X.-H. Wang, and Y.-W. Liu, "A survey on recent deep learning-driven singing voice synthesis systems," in *2021 IEEE International Conference on Artificial Intelligence and Virtual Reality (AIVR)*. IEEE, 2021, pp. 319–323.
- [12] F. Eyben, S. Buchholz, N. Braunschweiler, J. Latorre, V. Wan, M. J. Gales, and K. Knill, "Unsupervised clustering of emotion and voice styles for expressive tts," in *ICASSP 2012 IEEE International Conference on Acoustics, Speech and Signal Processing (ICASSP)*. IEEE, 2012, pp. 4009–4012.
- [13] Y. Wang, R. Skerry-Ryan, Y. Xiao, D. Stanton, J. Shor, E. Battenberg, R. Clark, and R. A. Saurous, "Uncovering latent style factors for expressive speech synthesis," *arXiv preprint arXiv:1711.00520*, 2017.
- [14] Y. Wang, D. Stanton, Y. Zhang, R.-S. Ryan, E. Battenberg, J. Shor, Y. Xiao, Y. Jia, F. Ren, and R. A. Saurous, "Style tokens: Unsupervised style modeling, control and transfer in end-to-end speech synthesis," in *Proceedings of the 35th International Conference on Machine Learning (ICML)*, vol. 80. Proceedings of Machine Learning Research, 2018, pp. 5180–5189.
- [15] R. Skerry-Ryan, E. Battenberg, Y. Xiao, Y. Wang, D. Stanton, J. Shor, R. Weiss, R. Clark, and R. A. Saurous, "Towards end-to-end prosody transfer for expressive speech synthesis with tacotron," in *Proceedings of the 35th International Conference on Machine Learning (ICML)*, vol. 80. Proceedings of Machine Learning Research, 2018, pp. 4693–4702.
- [16] V. Wan, C.-A. Chan, T. Kenter, J. Vit, and R. Clark, "Chive: Varying prosody in speech synthesis with a linguistically driven dynamic hierarchical conditional variational network," in *Proceedings of the 36th International Conference on Machine Learning (ICML)*. Proceedings of Machine Learning Research, 2019, pp. 5806–5815.
- [17] R. Valle, J. Li, R. Prenger, and B. Catanzaro, "Mellotron: Multispeaker expressive voice synthesis by conditioning on rhythm, pitch and global style tokens," in *ICASSP 2020 IEEE International Conference on Acoustics, Speech and Signal Processing (ICASSP)*. IEEE, 2020, pp. 6189–6193.
- [18] S.-Y. Um, S. Oh, K. Byun, I. Jang, C. Ahn, and H.-G. Kang, "Emotional speech synthesis with rich and granularized control," in *ICASSP 2020 IEEE International Conference on Acoustics, Speech and Signal Processing (ICASSP)*. IEEE, 2020, pp. 7254–7258.
- [19] B. Schnell and P. N. Garner, "Improving emotional tts with an emotion intensity input from unsupervised extraction," in *Proceedings of 11th ISCA Speech Synthesis Workshop (SSW 11)*, 2021, pp. 60–65.
- [20] C.-B. Im, S.-H. Lee, S.-B. Kim, and S.-W. Lee, "Emoq-tts: Emotion intensity quantization for fine-grained controllable emotional text-to-speech," in *ICASSP 2022-2022 IEEE International Conference on Acoustics, Speech and Signal Processing (ICASSP)*. IEEE, 2022, pp. 6317–6321.
- [21] T. Saitou, M. Unoki, and M. Akagi, "Extraction of f0 dynamic characteristics and development of f0 control model in singing voice," in *Proceedings of International Community For Auditory Display, ICAD, 2002*, pp. 0–3.
- [22] Y. Xue, Y. Hamada, and M. Akagi, "Emotional speech synthesis system based on a three-layered model using a dimensional approach," in *2015 Asia-Pacific Signal and Information Processing Association Annual Summit and Conference (APSIPA)*. IEEE, 2015, pp. 505–514.
- [23] T.-H. Nguyen and M. Akagi, "Synthesis of expressive singing voice by f0, amplitude envelope and spectral feature conversion," in *2018 RISP International Workshop on Nonlinear Circuits, Communications and Signal Processing (NCSP2018)*. Research Institute of Signal Processing, Japan, 2018.
- [24] K. R. Scherer, J. Sundberg, B. Fantini, S. Trznadel, and F. Eyben, "The expression of emotion in the singing voice: Acoustic patterns in vocal performance," *The Journal of the Acoustical Society of America*, vol. 142, no. 4, pp. 1805–1815, 2017.
- [25] L.-C. Chen, G. Papandreou, I. Kokkinos, K. Murphy, and A. L. Yuille, "DeepLab: Semantic image segmentation with deep convolutional nets, atrous convolution, and fully connected crfs," *IEEE transactions on pattern analysis and machine intelligence*, vol. 40, no. 4, pp. 834–848, 2017.
- [26] A. Vaswani, N. Shazeer, N. Parmar, J. Uszkoreit, L. Jones, A. N. Gomez, L. Kaiser, and I. Polosukhin, "Attention is all you need," in *Advances in Neural Information Processing Systems (NeurIPS)*, vol. 30. Neural information processing systems foundation, 2017, pp. 5998–6008.
- [27] M. Nishimura, K. Hashimoto, K. Oura, Y. Nankaku, and K. Tokuda, "Singing voice synthesis based on deep neural networks," in *Proceedings of the Annual Conference of the International Speech Communication Association (INTERSPEECH)*, vol. 2016, 2016, pp. 2478–2482.
- [28] Y. Ren, Y. Ruan, X. Tan, T. Qin, S. Zhao, Z. Zhao, and T.-Y. Liu, "FastSpeech: Fast, robust and controllable text to speech," in *Advances in Neural Information Processing Systems (NeurIPS)*, vol. 32. Neural information processing systems foundation, 2019.
- [29] P. Chandna, M. Blaauw, J. Bonada, and E. Gómez, "Wgansing: A multi-voice singing voice synthesizer based on the wasserstein-gan," in *2019 27th European Signal Processing Conference (EUSIPCO)*. IEEE, 2019, pp. 1–5.
- [30] Y. Hono, K. Hashimoto, K. Oura, Y. Nankaku, and K. Tokuda, "Singing voice synthesis based on generative adversarial networks," in *ICASSP 2019 IEEE International Conference on Acoustics, Speech and Signal Processing (ICASSP)*. IEEE, 2019, pp. 6955–6959.
- [31] S. Sankaran, S. Nanjundan, and G. P. Anand, "Anyone gan sing," *arXiv preprint arXiv:2102.11058*, 2021.
- [32] A. Gibiansky, S. Arik, G. Diamos, J. Miller, K. Peng, W. Ping, J. Raiman, and Y. Zhou, "Deep voice 2: Multi-speaker neural text-to-speech," vol. 30. Neural information processing systems foundation, 2017.
- [33] M. Chen, X. Tan, Y. Ren, J. Xu, H. Sun, S. Zhao, T. Qin, and T.-Y. Liu, "Multispeech: Multi-speaker text to speech with transformer," *arXiv preprint arXiv:2006.04664*, 2020.
- [34] L. Zhang, C. Yu, H. Lu, C. Weng, C. Zhang, Y. Wu, X. Xie, Z. Li, and D. Yu, "Durian-sc: Duration informed attention network based singing voice conversion system," in *Proceedings of the Annual Conference of*

- the International Speech Communication Association (INTERSPEECH)*, vol. 2020, 2020, pp. 1231–1235.
- [35] S. Wang, J. Liu, Y. Ren, Z. Wang, C. Xu, and Z. Zhao, “Mr-svs: Singing voice synthesis with multi-reference encoder,” *arXiv preprint arXiv:2201.03864*, 2022.
- [36] M. Blaauw, J. Bonada, and R. Daido, “Data efficient voice cloning for neural singing synthesis,” in *ICASSP 2019 IEEE International Conference on Acoustics, Speech and Signal Processing (ICASSP)*. IEEE, 2019, pp. 6840–6844.
- [37] J. Lee, H.-S. Choi, and K. Lee, “Expressive singing synthesis using local style token and dual-path pitch encoder,” *arXiv preprint arXiv:2204.03249*, 2022.
- [38] T. Hakanpää, T. Waaramaa, and A.-M. Laukkanen, “Training the vocal expression of emotions in singing: Effects of including acoustic research-based elements in the regular singing training of acting students,” *Journal of Voice*, 2021.
- [39] T. Li, S. Yang, L. Xue, and L. Xie, “Controllable emotion transfer for end-to-end speech synthesis,” in *2021 12th International Symposium on Chinese Spoken Language Processing (ISCSLP)*. IEEE, 2021, pp. 1–5.
- [40] H. Choi, S. Park, J. Park, and M. Hahn, “Multi-speaker emotional acoustic modeling for cnn-based speech synthesis,” in *ICASSP 2019-2019 IEEE International Conference on Acoustics, Speech and Signal Processing (ICASSP)*. IEEE, 2019, pp. 6950–6954.
- [41] X. Zhu, Y. Lei, K. Song, Y. Zhang, T. Li, and L. Xie, “Multi-speaker expressive speech synthesis via multiple factors decoupling,” *arXiv preprint arXiv:2211.10568*, 2022.
- [42] C. Lu, X. Wen, R. Liu, and X. Chen, “Multi-speaker emotional speech synthesis with fine-grained prosody modeling,” in *ICASSP 2021 IEEE International Conference on Acoustics, Speech and Signal Processing (ICASSP)*. IEEE, 2021, pp. 5729–5733.
- [43] T. Li, X. Wang, Q. Xie, Z. Wang, and L. Xie, “Cross-speaker emotion disentangling and transfer for end-to-end speech synthesis,” *IEEE/ACM Transactions on Audio, Speech, and Language Processing*, vol. 30, pp. 1448–1460, 2022.
- [44] W.-N. Hsu, Y. Zhang, R. J. Weiss, H. Zen, Y. Wu, Y. Wang, Y. Cao, Y. Jia, Z. Chen, J. Shen *et al.*, “Hierarchical generative modeling for controllable speech synthesis,” *arXiv preprint arXiv:1810.07217*, 2018.
- [45] X. An, Y. Wang, S. Yang, Z. Ma, and L. Xie, “Learning hierarchical representations for expressive speaking style in end-to-end speech synthesis,” in *2019 IEEE Automatic Speech Recognition and Understanding Workshop (ASRU)*. IEEE, 2019, pp. 184–191.
- [46] G. Sun, Y. Zhang, R. J. Weiss, Y. Cao, H. Zen, and Y. Wu, “Fully-hierarchical fine-grained prosody modeling for interpretable speech synthesis,” in *ICASSP 2020-2020 IEEE international conference on acoustics, speech and signal processing (ICASSP)*. IEEE, 2020, pp. 6264–6268.
- [47] M. Kang, S. Kim, and I. Kim, “Unitts: Residual learning of unified embedding space for speech style control,” *arXiv preprint arXiv:2106.11171*, 2021.
- [48] Y. Lee and T. Kim, “Robust and fine-grained prosody control of end-to-end speech synthesis,” in *ICASSP 2019-2019 IEEE International Conference on Acoustics, Speech and Signal Processing (ICASSP)*. IEEE, 2019, pp. 5911–5915.
- [49] Y. Ren, C. Hu, X. Tan, T. Qin, S. Zhao, Z. Zhao, and T.-Y. Liu, “Fastspeech 2: Fast and high-quality end-to-end text to speech,” *9th International Conference on Learning Representations (ICLR)*, 2021.
- [50] Y. Hono, K. Hashimoto, K. Oura, Y. Nankaku, and K. Tokuda, “Sinsy: A deep neural network-based singing voice synthesis system,” *IEEE/ACM Transactions on Audio, Speech, and Language Processing*, vol. 29, pp. 2803–2815, 2021.
- [51] P. Wu, Z. Ling, L. Liu, Y. Jiang, H. Wu, and L. Dai, “End-to-end emotional speech synthesis using style tokens and semi-supervised training,” in *2019 Asia-Pacific Signal and Information Processing Association Annual Summit and Conference (APSIPA ASC)*. IEEE, 2019, pp. 623–627.
- [52] X. Wang, R. Girshick, A. Gupta, and K. He, “Non-local neural networks,” in *Proceedings of the IEEE conference on computer vision and pattern recognition*, 2018, pp. 7794–7803.
- [53] W. Han, Z. Zhang, Y. Zhang, J. Yu, C.-C. Chiu, J. Qin, A. Gulati, R. Pang, and Y. Wu, “Contextnet: Improving convolutional neural networks for automatic speech recognition with global context,” *arXiv preprint arXiv:2005.03191*, 2020.
- [54] S. Woo, D. Kim, J.-Y. Lee, and I. S. Kweon, “Global context and geometric priors for effective non-local self-attention,” 2021.
- [55] W. Luo, Y. Li, R. Urtasun, and R. Zemel, “Understanding the effective receptive field in deep convolutional neural networks,” *Advances in neural information processing systems*, vol. 29, 2016.
- [56] M. Cuturi and M. Blondel, “Soft-dtw: a differentiable loss function for time-series,” in *International conference on machine learning*. PMLR, 2017, pp. 894–903.
- [57] S. Choi, W. Kim, S. Park, S. Yong, and J. Nam, “Children’s song dataset for singing voice research,” in *The 21th International Society for Music Information Retrieval Conference (ISMIR)*. International Society for Music Information Retrieval, 2020.
- [58] J. Kim, J. Kong, and J. Son, “Conditional variational autoencoder with adversarial learning for end-to-end text-to-speech,” in *International Conference on Machine Learning*. PMLR, 2021, pp. 5530–5540.
- [59] M. Fréchet, “Sur la distance de deux lois de probabilité,” *Comptes Rendus Hebdomadaires des Seances de L Academie des Sciences*, vol. 244, no. 6, pp. 689–692, 1957.



Sungjae Kim received the B.S. and M.S. degree in CSEE (Computer Science and Electrical Engineering) at Handong Global University. He is currently a Ph.D student in CSEE at Handong Global University. Since 2019, he is a student researcher at DL-LAB of Handong Global University, working under the supervision of Prof. Injung Kim. His research interest includes deep learning, speech synthesis, singing voice synthesis, and speech recognition.

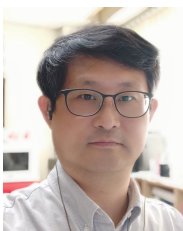


Yewon Kim received the B.S. degree in CSEE at Handong Global University. She is currently a M.S. student in CSEE at Handong Global University. From 2020 to June 2022, she worked as a student researcher at HAIL(Handong AI Lab) of Handong Global University with Prof. Charmgil Hong, participating in several industry projects as a student researcher. Since July 2022, she is a student researcher at DL-LAB of Handong Global University, working under the supervision of Prof. Injung Kim, participating projects related to speech synthesis and singing voice synthesis. Her research interest includes speech synthesis, singing voice synthesis and deep learning.

singing voice synthesis. Her research interest includes speech synthesis, singing voice synthesis and deep learning.



Jewoo Jun is currently a B.S. student in CSEE at Handong Global University. From 2022, he is a student researcher at DL-LAB of Handong Global University, working under the supervision of Prof. Injung Kim. His research interests include speech synthesis and singing voice synthesis.



Injung Kim is a professor of CSEE, Handong Global University since 2006. He received B.S., M.S., and Ph.D. degrees in Computer Science from KAIST (Korea Advanced Institute of Science and Technology). He was a senior research engineer of Inzisoft. He was the Head of the School of CSEE, Program Director of the CS major, and an AI advisor of Samsung SW Center and POSCO, and currently, he is research advisor of multiple AI companies. His research interests include deep learning, image analysis and synthesis, speech synthesis, data analysis and prediction, recommendation system, outlier detection, and natural language processing.

ysis and prediction, recommendation system, outlier detection, and natural language processing.